Downloaded from www.genesdev.org on May 17, 2006

The chicken talpid3 gene encodesa novel protein essentialfor Hedgehog signaling

Megan G. Davey, I. Robert Paton, Yili Yin, Maike Schmidt, Fiona K. Bangs, David R. Morrice, Terence Gordon Smith, Paul Buxton, Despina Stamataki, Mikiko Tanaka, Andrea E. Münsterberg, James Briscoe, Cheryll Tickle and Dave W. Burt

Genes & Dev. 2006 20: 1365-1377
doi:10.1101/gad.369106

Supplementary data *"Supplemental Research Data"*
http://www.genesdev.org/cgi/content/full/20/10/1365/DC1

References This article cites 37 articles, 14 of which can be accessed free at:
http://www.genesdev.org/cgi/content/full/20/10/1365#References

Email alerting service Receive free email alerts when new articles cite this article - sign up in the box at the top right corner of the article or **click here**

Notes

To subscribe to *Genes and Development* go to:
http://www.genesdev.org/subscriptions/

© 2006 Cold Spring Harbor Laboratory Press

Downloaded from www.genesdev.org on May 17, 2006

The chicken *talpid*^{3} gene encodes a novel protein essential for Hedgehog signaling

Megan G. Davey,[1,2] I. Robert Paton,[2] Yili Yin,[1] Maike Schmidt,[1] Fiona K. Bangs,[1] David R. Morrice,[2] Terence Gordon Smith,[1] Paul Buxton,[3] Despina Stamataki,[4] Mikiko Tanaka,[1] Andrea E. Münsterberg,[1,5] James Briscoe,[4] Cheryll Tickle,[1,6] and Dave W. Burt[2,7]

[1]Division of Cell and Developmental Biology, Wellcome Trust Biocentre (WTB), University of Dundee, Dundee DD1 5EH, United Kingdom; [2]Department of Genetics and Genomics, Roslin Institute (Edinburgh), Midlothian EH25 9PS, United Kingdom; [3]Division of Biomaterials and Tissue Engineering, Eastman Dental Institute, London WC1X 8LD, United Kingdom; [4]Division of Developmental Neurobiology, National Institute for Medical Research, London NW7 1AA, United Kingdom; [5]School of Biological Sciences, University of East Anglia, Norwich NR4 7TJ, United Kingdom

***Talpid*^{3} is a classical chicken mutant with abnormal limb patterning and malformations in other regions of the embryo known to depend on Hedgehog signaling. We combined the ease of manipulating chicken embryos with emerging knowledge of the chicken genome to reveal directly the basis of defective Hedgehog signal transduction in *talpid*^{3} embryos and to identify the *talpid*^{3} gene. We show in several regions of the embryo that the *talpid*^{3} phenotype is completely ligand independent and demonstrate for the first time that *talpid*^{3} is absolutely required for the function of both Gli repressor and activator in the intracellular Hedgehog pathway. We map the *talpid*^{3} locus to chromosome 5 and find a frameshift mutation in a KIAA0586 ortholog (ENSGALG00000012025), a gene not previously attributed with any known function. We show a direct causal link between KIAA0586 and the mutant phenotype by rescue experiments. KIAA0586 encodes a novel protein, apparently specific to vertebrates, that localizes to the cytoplasm. We show that Gli3 processing is abnormal in *talpid*^{3} mutant cells but that Gli3 can still translocate to the nucleus. These results suggest that the *talpid*^{3} protein operates in the cytoplasm to regulate the activity of both Gli repressor and activator proteins.**

[*Keywords*: Gli; Hedgehog signaling; chicken; *talpid*^{3}]

Supplemental material is available at http://www.genesdev.org.

Received October 6, 2005; revised version accepted March 9, 2006.

The chicken embryo has served as a powerful and influential model system. The recent completion of the chicken genome (International Chicken Genome Sequencing Consortium 2004) allows new opportunities to exploit the ease of manipulating chick embryos to study vertebrate development. A number of chicken mutants have arisen spontaneously, often in agricultural flocks where they were noticed because of reduced hatchability. *Talpid*^{3} is one such mutant (Hunton 1960), and is a member of the classical developmental *talpid* group, so called because their paddle-shaped limbs resemble those of the mole (*Talpa*). In the *talpid*^{3} mutant, besides limb defects, there is an almost bewildering set of malformations including face, skeleton, and vascular defects (Ede and Kelly 1964a,b; Hinchliffe and Ede 1968). It is now clear that all these abnormalities are in regions of the embryo that depend on Hedgehog (Hh) signaling (Ingham and McMahon 2001).

An intriguing feature of *talpid*^{3} is that some aspects of the gross phenotype (e.g., polydactylous limbs) suggest a gain of Hh function whereas others (e.g., hypoteleorism in which the eyes are pulled together) suggest a loss of function. Analysis of Hh target gene expression in both limb and face shows that, even within one region, some targets are expressed at abnormally low levels while others are expressed ectopically (Izpisua-Belmonte et al. 1992; Francis-West et al. 1995; Lewis et al. 1999a; Buxton et al. 2004). These opposite changes in gene expression seen in *talpid*^{3} may reflect dual roles of the Gli transcriptional effectors of Hh signaling, which can act as either activators (A) or repressors (R) (Ruiz i Altaba et al. 2003). There are three Gli proteins, Gli1, Gli2, and Gli3. Experiments in mice show that Gli3 but not Gli1 or Gli2 is required for limb patterning (Bai et al. 2002). In normal chick limb buds, Sonic hedgehog (Shh) produced posteriorly diffuses across the bud and prevents processing of full-length Gli3 protein to a short repressor form

Corresponding authors.
[6]E-MAIL c.a.tickle@dundee.ac.uk; FAX 44-1382-385-386
[7]E-MAIL Dave.Burt@bbsrc.ac.uk; FAX 44-131-440-0434.
Article and publication are at http://www.genesdev.org/cgi/doi/10.1101/gad.369106.

Downloaded from www.genesdev.org on May 17, 2006

(Gli3R). This results in low levels of full-length Gli3 protein that, together with other Gli proteins, can act as a transcriptional activator (Gli3A) and a gradient of Gli3R, highest anteriorly (Wang et al. 2000). Absence of high-level expression of some target genes in the posterior of *talpid*^{3} limb buds (e.g., *Ptc1*) and the inability to rescue their expression through the addition of Shh protein (Lewis et al. 1999a) suggests that GliA function is defective. Ectopic expression of other target genes in the anterior of *talpid*^{3} limb buds suggests that Gli3R levels are reduced anteriorly. The absence of high-level expression of *Ptc*, which encodes the Shh receptor and binds Shh, could lead to widespread diffusion of Shh ligand, reducing Gli3R levels. However, the limbs of Gli3$^{-/-}$ and Shh$^{-/-}$, Gli3$^{-/-}$ mutant mice, like those of *talpid*^{3} chick embryos, are polydactylous, with many unpatterned digits, and also show ectopic expression of Hh target genes (Hui and Joyner 1993; Litingtung et al. 2002; te Welscher et al. 2002).

Here we show that ectopic gene expression in *talpid*^{3} limb buds is ligand independent and assess the distribution of Gli3A versus Gli3R. The dorsoventral pattern of the neural tube in chick has been shown to depend on a balance between GliA and GliR function (Persson et al. 2002; Stamataki et al. 2005). We explore whether the *talpid*^{3} mutation compromises both GliA and GliR function in dorsoventral patterning of the neural tube and adjacent somites. We rescue Gli function by electroporation into the *talpid*^{3} neural tube. We then combine knowledge of the chicken genome with the manipulability of chick embryos to identify the *talpid*^{3} gene and carry out functional complementation tests within the mutant neural tube to confirm identification unequivocally. We show that the *talpid*^{3} protein localizes to the cytoplasm and that although Gli3 processing is abnormal in mutant chick cells, both Gli3A and Gli3R can still translocate to the nucleus. We conclude that the *talpid*^{3} protein acts in the cytoplasm to regulate the functional activity of both the repressor and activator forms of Gli.

Results

Basis of the talpid^3 *limb polydactyly*

The polydactylous phenotype of *talpid*^{3} limbs suggests a gain of Hh function. Comparison of stage 19 Hamburger Hamilton (HH) (Hamburger and Hamilton 1951) limb buds using immunohistochemistry showed that Shh protein is more widespread in *talpid*^{3} (Fig. 1A,B). In Western blots, more Shh protein was found in the middle third of *talpid*^{3} limb buds than in wild type (Fig. 1C). To test whether ectopic gene expression in *talpid*^{3} limb buds is dependent on this ectopic Shh protein, we attempted to rescue the mutant phenotype by inhibiting Shh signaling or removing its source; we monitored rescue by examining *Hoxd13* expression, which is ectopically expressed throughout *talpid*^{3} limb buds instead of being posteriorly restricted (Izpisua-Belmonte et al. 1992). We applied cyclopamine, which inhibits Smo activity (Frank-Kamenetsky et al. 2002) to stage 17 HH wing buds. In 5/6 treated *talpid*^{3} wings, *Hoxd13* expression was still strongly expressed (Fig. 1E; right wing bud) whereas, in 3/4 treated wild-type wings, expression was much reduced (Fig. 1D; right wing bud). Expression of *Hoxd13* was retained in most cases in wings treated with ethanol (4/5 wild-type, 3/3 *talpid*^{3}) (data not shown). We also removed future *Shh* expressing cells at stage 16 HH. This had no effect on *Hoxd13* expression in *talpid*^{3} wing buds (3/3) (Fig. 1G; right wing bud) but, in wild type, expression was reduced or abolished (7/7) (Fig. 1F; right wing bud). These results show that, although Shh protein is more widely distributed in *talpid*^{3} limb buds, ectopic *Hoxd13* expression is ligand independent.

Analysis of gene expression in *talpid*^{3} limb buds and the fact that these changes in expression are ligand independent suggest that both GliA and GliR functions are defective. In order to assess the levels of the different forms of Gli proteins, we extracted proteins from the anterior, middle, and posterior thirds of *talpid*^{3} buds (either wing or leg) and carried out Western blot analysis using an antibody against Gli3 that recognizes both the full-length form, Gli3A (190 kDa) and the processed short form, Gli3R (83 kDa). We then compared the levels of the two forms of Gli3 with those seen in wild-type limb buds by carrying out analysis on either wing buds or leg buds. We present the data in histograms for the wing buds and show the Western blot for the leg buds. In the wild-type limb buds, we detected both Gli3A and Gli3R forms (Fig. 1H,I) and, as previously reported (Wang et al. 2000), Gli3R is present in a gradient along the anterior–posterior axis with maximal levels of Gli3R in the anterior region of the bud (Fig. 1H,I). In contrast, in *talpid*^{3} wing buds (Fig. 1I), levels of Gli3A are strikingly increased and the polarized distribution of Gli3R is abolished. Western blots of Gli3 in *talpid*^{3} leg buds (Fig. 1H) also confirmed that Gli3R is not graded and, in addition, that Gli3A levels are strikingly elevated. We also carried out Western blot analysis on extracts from whole limb buds (both wing and leg pooled together) from wild-type and *talpid*^{3} embryos and estimated the Gli3A/Gli3R ratio (Fig. 1J). This analysis shows that this ratio is strikingly elevated in the mutant. Furthermore, we found that the ratio of Gli3A/Gli3R was also elevated in extracts from *talpid*^{3} trunk, which includes other tissues, such as neural tube and somites, that are patterned by Hh signaling. Thus there is a generalized defect in Gli3 processing in *talpid*^{3} embryos that leads to high levels of activator compared with repressor.

Patterning of talpid^3 *neural tube and somite*

Floor plate and associated Shh signaling is markedly reduced in *talpid*^{3} neural tube of stage 20 embryos. *Shh* transcripts and protein are expressed in *talpid*^{3} notochord, as in wild-type embryos, but are extremely patchy or completely absent in floor plate (Fig. 2, cf. A1,B1 and A2,B2). In wild-type embryos, floor plate is also characterized by Shh-dependent HNF3β/FoxA2 expression (Fig. 2D1), which is either very reduced or absent in *talpid*^{3}

Downloaded from www.genesdev.org on May 17, 2006

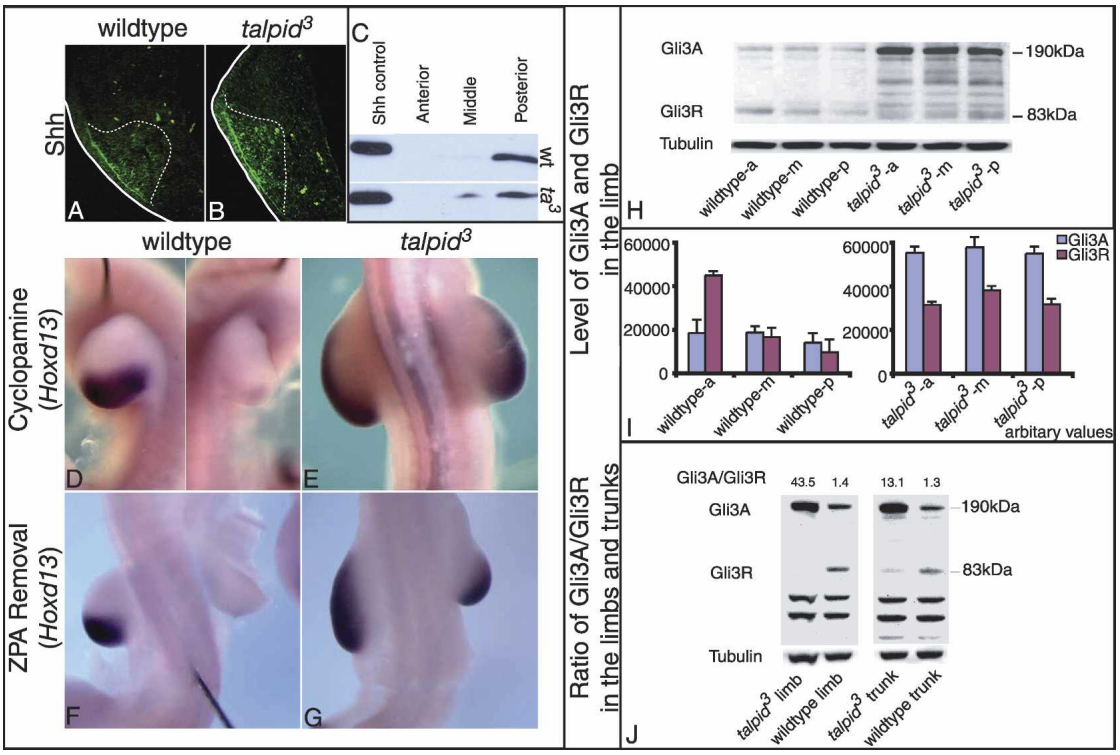

Figure 1. Localization of Shh protein, effects of reducing Shh activity in wild-type and *talpid*^{3} limb buds, and status of Gli3 protein. (*A*,*B*) Localization of Shh protein in stage 19 HH wild-type (*A*) and *talpid*^{3} (*B*) limb buds. Dotted lines indicate limit of staining. (*C*) Western blot analysis of Shh protein in different regions (anterior, middle, posterior) of stage 20 HH wild-type (wt) and *talpid*^{3} (*ta*^{3}) limbs. (*D*,*E*) *Hoxd13* expression in wild-type (*D*) and *talpid*^{3} (*E*) right limbs treated with cyclopamine compare with control left limbs. (*F*,*G*) *Hoxd13* expression in wild-type (*F*) and *talpid*^{3} (*G*) right limbs after removal of posterior mesenchyme; compare with control left limbs. (*H*,*I*) Status of Gli3 protein in different regions (anterior, a; middle, m; posterior, p) of stage 24 wild-type and *talpid*^{3} limb buds. (*H*) Immunoblot shows levels of Gli3A and Gli3R in wild-type and *talpid*^{3} legs ($n > 3$). (*I*) Histograms show levels of Gli3 proteins in wild-type and *talpid*^{3} wing buds; standard deviations shown, $n = 3$. (*J*) Immunoblot directly compares levels of Gli3 protein in wild-type and *talpid*^{3} limbs and trunk tissue. Numbers at *top* of each lane show ratios of Gli3A/Gli3R. *H* and *J* also illustrate tubulin loading controls.

(Fig. 2D2). High-level expression of *Ptc1* or *Ptc2* genes, considered to be a direct readout of Shh signaling (Pearse et al. 2001), is lost in *talpid*^{3} (Fig. 2, cf. C1 and C2; see Lewis et al. 1999a).

We characterized dorsoventral patterning of the neural tube in *talpid*^{3} embryos, investigating markers of chick neuronal identity that are established by Hh signaling, (Persson et al. 2002). We used embryos at stage 20 when the mutant phenotype is readily observable. In *talpid*^{3} expression of ventral markers, Nkx2.2 (p3 progenitor cells) (Fig. 2E2) and Islet2 (MNv) (Fig. 2G2) is almost lost completely while expression of Islet1 (MN) (Fig. 2F2, arrows indicating residual expression) and Lim3 (MN and V2) (Fig. 2H2, arrow indicating residual expression) is either lost or expressed in only a few ventrally located midline cells. Expression of intermediate markers, Pax6 (Fig. 2I2) and *Dbx2* (Fig. 2J2) extends into the ventral-most region of the neural tube, and Lim1/2-positive cells, normally located in a stereotypical pattern in the intermediate-dorsal region (Fig. 2K1), are found more ventrally and wild-type pattern is lost (Fig. 2K2). En1 expressing cells (V1) (Fig. 2L1, bracket) are also shifted ventrally and distributed more widely (Fig. 2L2, bracket). Expression of dorsal markers *Gsh1* and Pax7 is expanded ventrally (Fig. 2M2,N2) with Pax7, normally expressed in dorsal third (Fig. 2N1), being expressed in dorsal half of *talpid*^{3} neural tube (Fig. 2N2) and the band of *Gsh1* expression being broader (Fig. 2M2, bracket).

In summary, in *talpid*^{3} there is a loss and/or reduction of ventral genes (*talpid*^{3}, Fig. 2O, regions A and B) accompanied by ventral expansion of genes normally expressed in dorsal neural tube, suggesting a loss of Hedgehog function and failure of Gli activator. Expansion of intermediate neural (*talpid*^{3}, Fig. 2O, region C) tube genes more ventrally suggests a loss of Gli repressor.

We examined dorsoventral patterning of somites, which is controlled by Shh from notochord and floor plate in the chick, mouse, and zebrafish (Munsterberg et al. 1995; Borycki et al. 1999; Lewis et al. 1999b). As in neural tube, there is low-level *Ptc2* expression throughout *talpid*^{3} somites (Fig. 2C2, arrow). In *talpid*^{3}, *Pax1* is expressed more widely than in wild type (Fig. 3A) and positive cells are found displaced dorsally between myotome and dermomyotome (Fig. 3B, arrow) instead of be-

Downloaded from www.genesdev.org on May 17, 2006

ing clearly demarcated from myotome expressing *MyoD*. The dermomyotome expresses *Pax3* (Fig. 3C) and double in situ hybridization showed that, in *talpid*^{3} rostral somites, epithelial cells in dermomyotome express *Myo*D (Fig. 3D, arrow). Expansion of *MyoD* into more dorsal regions can be mimicked by overexpression of Shh in wild-type somites (Fig. 3E, arrow). Thus expansion and shift of cell types into more dorsal domains in *talpid*^{3} somites seems to resemble a gain of Hh function. To establish whether the effects of the mutation are autonomous, undifferentiated somites taken from the tail region of a stage 20 HH *talpid*^{3} embryo were implanted into stage 10–12 HH wild-type hosts. Widespread expression of *MyoD* in *talpid*^{3}-derived somites was still seen (Fig. 3F, arrow) even in a wild-type environment. This suggests that gain of function in somite, as in limb, is more likely due to a defect in Hh signaling in responding cells than to ectopic ligand.

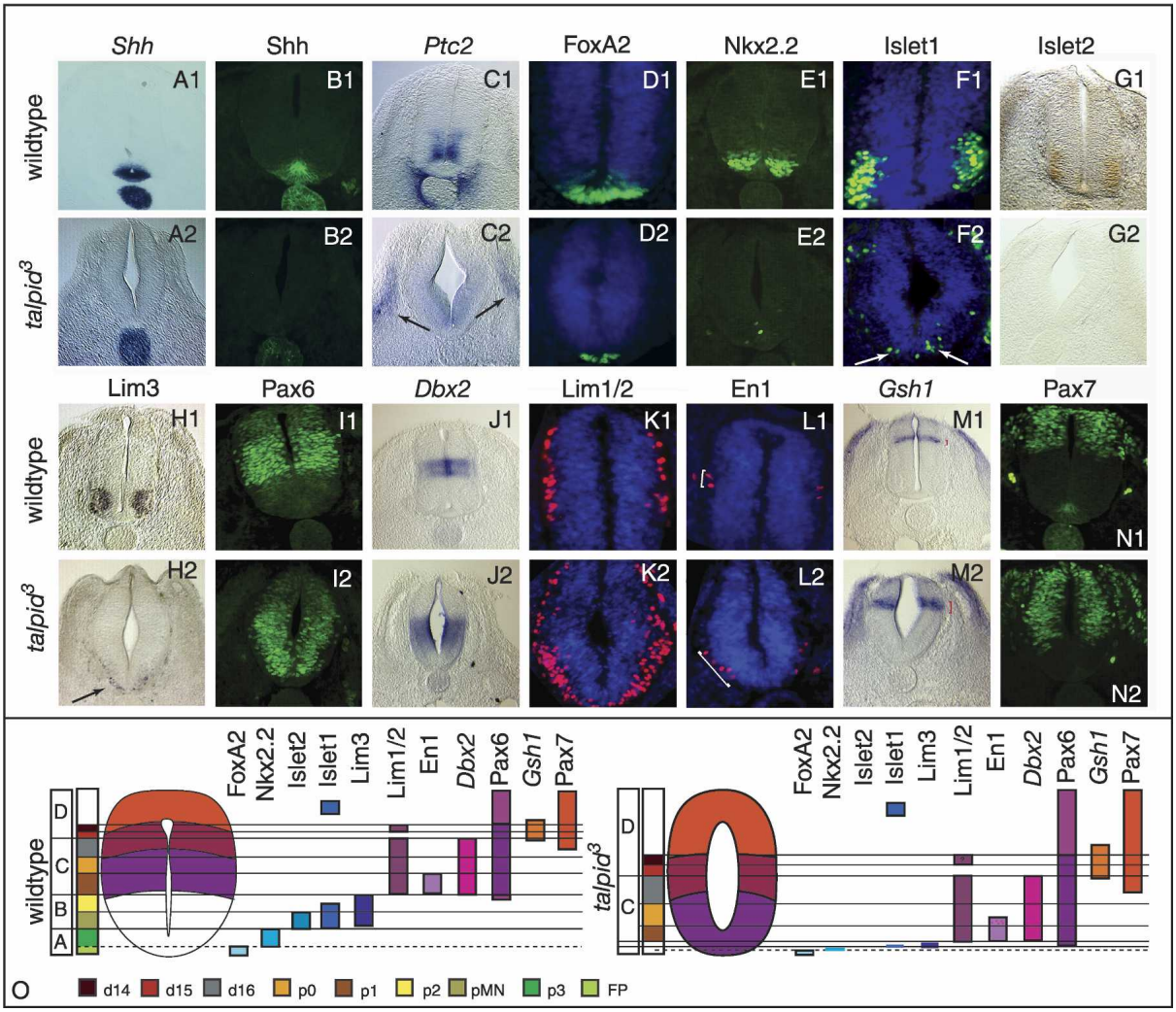

Figure 2. Expression of Shh and Shh-dependent genes in the dorsoventral axis of the neural tube in stage 20 HH wild-type and *talpid*^{3} embryos. *Shh* expressed in notochord and floor plate in wild-type (*A1*) and in notochord but not ventral neural tube in *talpid*^{3} (*A2*). Shh protein in notochord and floor plate in wild type (*B1*) but only in *talpid*^{3} notochord (*B2*). *Ptc2* expressed strongly around notochord and dorsal to floor plate in wild type (*C1*) but weakly in *talpid*^{3} neural tube and abnormally in somite (arrow, *C2*). HNF3β/FoxA2-positive cells in floor plate in wild type (*D1*); fewer HNF3β/FoxA2-positive cells indicate reduced floor plate in *talpid*^{3} (*D2*). Nkx2.2 expression in p3 progenitors in wild type (*E1*) and reduced or absent in *talpid*^{3} (*E2*). Islet1 expression in motorneurons in wild type (*F1*); reduced in *talpid*^{3}, remaining positive cells shown by arrows (*F2*). Islet2 expression in ventral motorneurons in wild type (*G1*) and absent in *talpid*^{3} (*G2*). Lim3 expression in p2 and motorneurons in wild type (*H1*); reduced in *talpid*^{3} (arrow, *H2*). Pax6 expression in wild type (*I1*) and *talpid*^{3} (*I2*). *Dbx2* expression in wild type (*J1*); ventrally expanded in *talpid*^{3} (*J2*). Lim1/2 expression in p1-d14 neurons in wild type (*K1*); ventralized in *talpid*^{3} (*K2*). En-1 expression in p1 neurons in wild type (*L1*); broader and ventralized (bracket) in *talpid*^{3} (*L2*). Stripe of *Gsh1* expression (bracket) in wild type (*M1*); expanded ventrally in *talpid*^{3} (*M2*; cf. brackets in *M1* and *M2*). Pax7 expression in wild type (*N1*); expanded ventrally in *talpid*^{3} (*N2*). (*O*) Summary of neuronal progenitor domains in neural tube of wild-type and *talpid*^{3} embryos. *A–D* represent areas of neural tube dependent on different Gli activities (Persson et al. 2002). *Talpid*^{3} embryos lack floor plate, motorneurons, and p3 and p2 neurons but have expanded p0-d14 domains.

Downloaded from www.genesdev.org on May 17, 2006

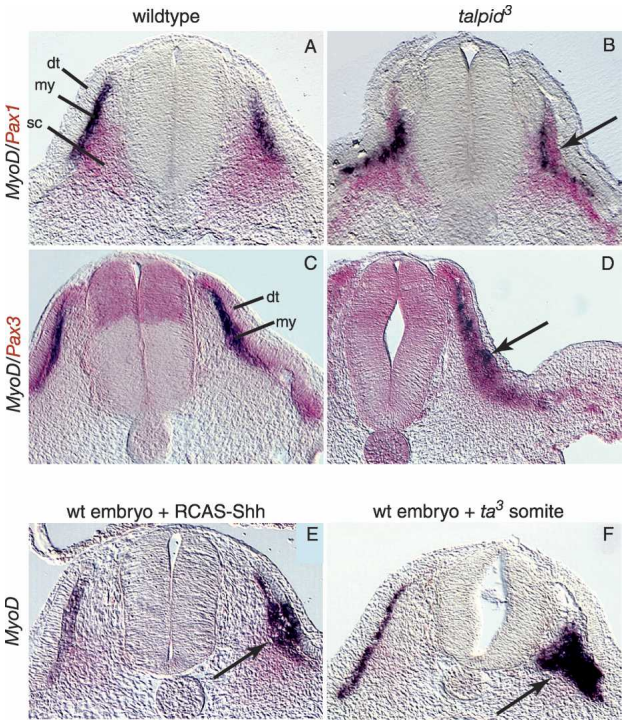

Figure 3. Expression of Shh-dependent genes in somites of the stage 20 HH wild-type and *talpid*^{3} embryos. *MyoD* (black) and *Pax1* (red) expression in wild-type (*A*) and *talpid*^{3} somites (*B*; arrow indicates abnormal *Pax1* localization). *MyoD* (black) and *Pax3* (red) expression in wild-type (*C*) and *talpid*^{3} somites (*D*; arrow indicates abnormal *MyoD* localization). (*E*) Wild-type embryo infected with pRCAS-Shh (*right* somite), showing ectopic *MyoD* expression. (*F*) *Talpid*^{3} somite (*right*) implanted in wild-type embryo, showing continued abnormal *MyoD* expression (arrow).

Rescue of talpid^3 *neural tube pattern*

Failure to produce ventral domains of progenitor neurons in *talpid*^{3} neural tube could be due to reduced Shh protein because there is no floor plate. We first tested this by implanting Shh-soaked beads or Shh-expressing cells into *talpid*^{3} neural tube and examining Islet1 expression. Twenty-four hours later, there was no rescue of Islet1 expression in *talpid*^{3} embryos (9/9) (Supplementary Fig. S6J2). Further experiments in *talpid*^{3} embryos showed that application of a Shh bead to the neural tube did not induce Nkx2.2 or high-level *Ptc1* expression or alter either Pax6 or Pax7 expression (Supplementary Fig. S6I2,K2,L2,M) as is seen in wild-type embryos treated with Shh (for details, see Fig. 7, below). These data show that Shh ligand cannot rescue dorsoventral patterning of the *talpid*^{3} neural tube and that a reduction in floor plate does not account for loss of ventral neurons.

Inability to rescue neural tube patterning with Shh suggests that *talpid*^{3} cells cannot transduce the Shh signal and that GliA does not function properly. To test this hypothesis directly, we electroporated neural tubes of stage 20 HH *talpid*^{3} and wild-type embryos with an activated Gli construct that can constitutively translocate to the nucleus (pCAGGS-Gli3A^{HIGH}) (Stamataki et al. 2005) and monitored dorsoventral gene expression. Cell-by-cell analysis showed that Nkx2.2 (Fig. 4E1,E2), Islet1 (Fig. 4F1,F2, arrows), and Lim3 expression (data not shown) was recovered in *talpid*^{3} embryos while expression of Lim1/2 (data not shown), Pax6 (Fig. 4G1,G2, arrows), and Pax7 (Fig. 4H1,H2, arrow) was reduced in cells expressing the pCAGGS-Gli3A^{HIGH} construct (2/2). In wild-type embryos, ectopic expression of Nkx2.2 (Fig. 4A1,A2, arrow), Islet1 (Fig. 4B1,B2, top arrow), and Lim3 (data not shown) was also induced and Pax6 (Fig. 4C1,C2, arrow) and Pax7 (Fig. 4D1,D2, arrow) expression reduced. Electroporation of control pCAGGS-eGFP into neural tube of either *talpid*^{3} or wild-type embryos produced no gene expression changes (data not shown). These results demonstrate directly that supplying *talpid*^{3} cells with functional activated Gli rescues the defect.

Genetic mapping and identification of talpid^3

Linkage analysis of 110 individual carriers mapped the *TA3* locus close to markers *ADL0298* and *ADL0166* on chromosome 5. Mapping further markers refined the location to an interval containing *COM0184*-(5.1)-*ADL0166*-(7.3)-*SIX4*-(3.6)-*DAAM1*-(0.9)-*TA3*-(4.6)-*OTX2*-(8.3)-*ADL0298*-(0.0)-*ROS0330*-(2.8)-*BMP4* (genetic distances between markers in centimorgans). We constructed a detailed physical map of this region to define gene content and develop more markers (Fig. 5A). Using these markers, the location of the *talpid*^{3} mutation was reduced to an interval encoding five genes: *KCNK16-DACT1-ENSGALG00000012025-TIMM9-ARID4A* (Fig. 5B).

To look for sequence changes that might identify the *talpid*^{3} mutation we sequenced cDNA clones derived from wild-type and *talpid*^{3} embryos (Supplementary Table S1). Sequence analysis of *talpid*^{3} *KIAA0586* cDNA revealed an insertion mutation of a single thymine residue (Fig. 5C), which was confirmed by sequencing genomic products from carrier and noncarriers (Supplementary Fig. S1). Translation from *KIAA0586* in *talpid*^{3} is terminated nine residues after the thymine insertion at a stop codon (Fig. 5C); this frameshift mutation is predicted to produce a truncated protein of 366 amino acids compared with 1524 in wild type (Fig. 6A). A multispecies comparison of *KIAA0586* orthologs (Supplementary Fig. S2) shows extensive homology across all 30 exons, and a number of highly conserved noncoding regions. The complete sequence of the chicken *KIAA0586* mRNA is shown in Supplementary Figure S3. The translation initiation codon at position 137 was selected as the most likely based on the longest open reading frame and homology with other vertebrate orthologs (Supplementary Fig. S4). To detect KIAA0586 orthologs in other species, we combined information from conservation of sequence and gene order (Supplementary Figs. S4, S5). Complete conservation of gene order was found for *DAAM1-DACT1-KIAA0586-TIMM9-ARID4A* in all vertebrates examined. No homologs were detected in *Ciona*

Downloaded from www.genesdev.org on May 17, 2006

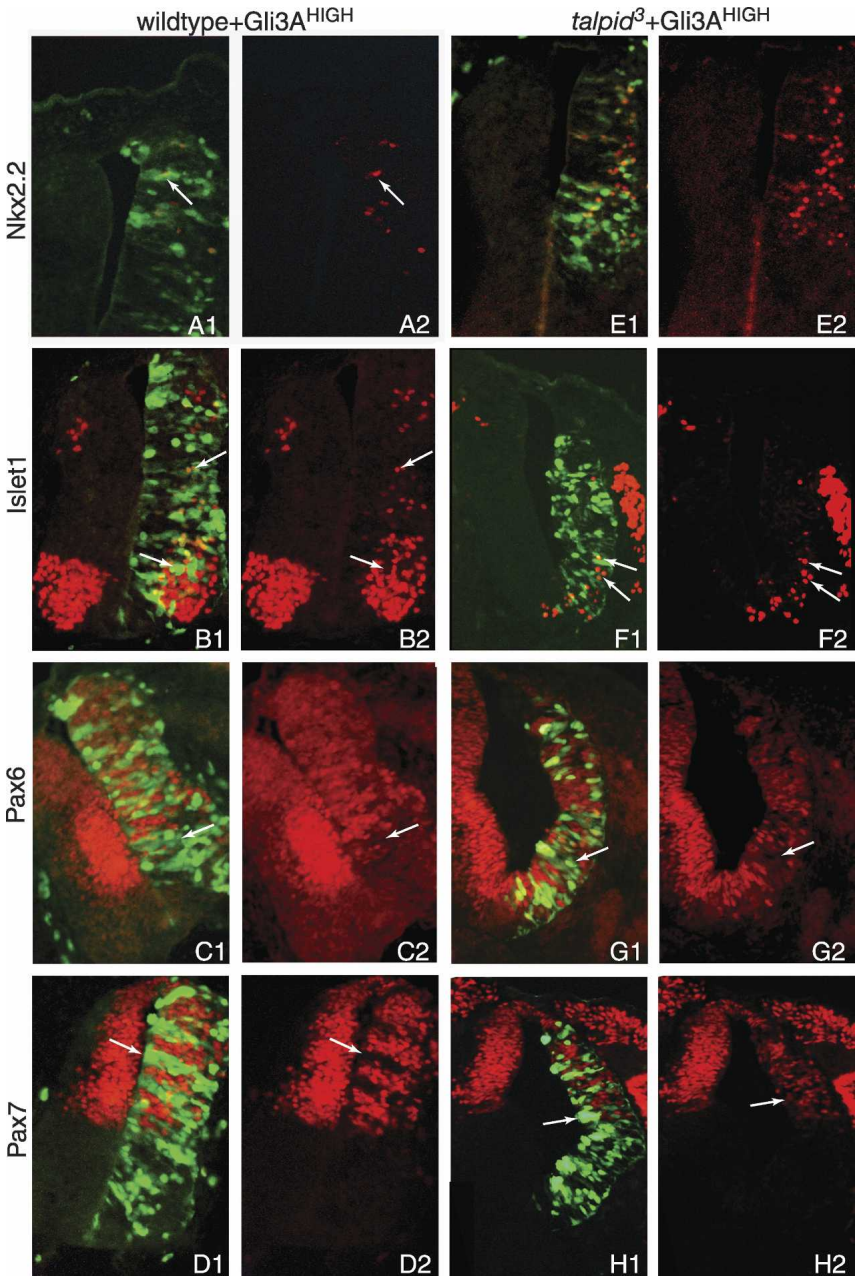

Figure 4. Rescue of *talpid*^{3} neural tube with activated Gli constructs. (*A–H*) Stage 20 HH wild-type and *talpid*^{3} embryos electroporated with Gli3A^{HIGH} (activated Gli construct). Green indicates expression of GFP in transfected cells; red indicates protein expression detected by immunohistochemistry. *A1–H1* are overlays of GFP and immunostaining; *A2–H2* are immunostaining alone. (*A–D*) Wild-type neural tube. Induction of Nkx2.2-positive cells (arrows, *A1*,*A2*); Islet1-positive cells (arrows, *B1*,*B2*). Down-regulation of Pax6 (arrow, *C1*,*C2*); Pax7 (*D1*,*D2*). (*E–H*) *talpid*^{3} neural tube. Induction of Nkx2.2-positive cells (*E1*,*E2*) and Islet1-positive cells (*upper* arrow, *F1*,*F2*). Down regulation of Pax6 (arrow, *G1*,*G2*); Pax7 (arrow, *H1*,*H2*).

intestinalis, *Drosophila melanogaster*, or *Caenorhabditis elegans*. Using *Codonml* (PAML 3.13) we were able to estimate the K_A/K_S ratio for KIAA0586 (~0.28), a measure of selection constraint (Yang and Nielsen 2000). For comparison, the K_A/K_S ratio for mammalian orthologous gene pairs (Rat Genome Sequencing Project Consortium 2004) was 0.09–0.11, most genes being under strong to moderate purifying selection. The K_A/K_S ratio for KIAA0596 indicates that this protein has been under reduced purifying selection and/or increased positive selection. No specific functional domains were predicted in the peptide sequence. Most highly conserved are three globular domains, coiled-coil regions, and a central region, with as yet, no known structural features, and least conserved is the C-terminal region (Fig. 6A).

Expression of talpid^3 *gene and protein and analysis of Gli3 translocation in mutant cells*

KIAA0586 is ubiquitously expressed in wild-type embryos (stages 12–35 HH), consistent with the *talpid*^{3} mutation affecting multiple tissues (Fig. 6B). Using the program *ProtComp*, the KIAA0586 protein was predicted to be cytoplasmic. In order to determine cellular localization experimentally, we expressed either C-terminal-tagged KIAA0586-myc or N-terminal-tagged KIAA0586-

Downloaded from www.genesdev.org on May 17, 2006

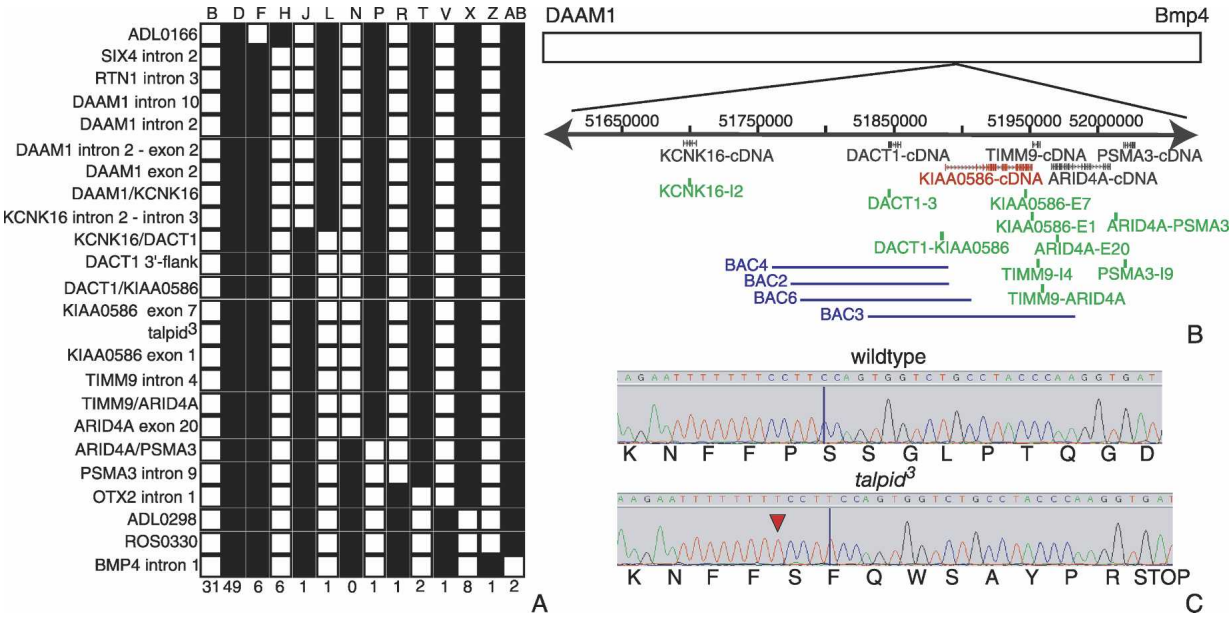

Figure 5. Mapping and identification of the *talpid*^{3} mutation in KIAA0586 (ENSGALG00000012025). (*A*) Results of typing backcross progeny. Values at *bottom* of figure are number of progeny inheriting chromosome 5 haplotypes from F_1 carrier parent. White squares indicate wild-type (*N*) allele; black squares indicate the *talpid*^{3} (*TA3*) allele. (*B*) Chromosomal organization of *TA3* locus relative to known genes. The *top* part of figure shows locations of bacterial artificial chromosomes, together with BLAST results using full-length cDNA sequences isolated in this region and markers used in genetic analysis. (*C*) Sequence trace files showing frameshift mutation in *TA3* compared with *N* alleles. Translation products of alleles are shown *below* DNA sequences; the effect of frameshift mutation (*TA3* allele) is shown as an altered amino sequence with an in-frame stop codon; details of marker sequences are in Supplementary Table S2.

HA in limb bud cells from wild-type chick embryos or in the chicken DFI cell line and visualized cellular localization by immunofluorescence. In all cases, labeling was confined to the cytoplasm (Fig. 6D,E), suggesting the *talpid*^{3} protein is a cytoplasmic protein.

To further investigate the role of KIAA0586 in Hh signaling, we compared intracellular localization of Gli3 in wild-type and *talpid*^{3} mutant chick limb bud cells. In one set of experiments, we isolated cytoplasmic and nuclear fractions from wild-type and mutant cells and then carried out Western blot analysis as before (Fig. 6F). We assessed the effectiveness of the fractionation by detecting tubulin and found this to be confined to the cytoplasmic fraction (Fig. 6F). Both full-length (190 kDa) and processed (83 kDa) Gli3 proteins were readily detected in nuclei isolated from wild-type chick limb bud cells but not in the cytoplasmic fraction. Both Gli3 forms were also detected in the nuclei of *talpid*^{3} cells, although full-length Gli3 could also be detected in the cytoplasm of mutant cells (Fig. 6F). Furthermore when the ratio of Gli3A/Gli3R was compared, it is evident that *talpid*^{3} cells from limb and head have a much higher ratio of Gli3A/Gli3R in the nucleus (Fig. 6G) than wild-type cells. We also expressed pGli3-myc in wild-type and *talpid*^{3} chick limb bud cells and visualized localization using immunofluorescence (Fig. 6H). Localization of Gli3-myc was rather variable but was seen in both nucleus and cytoplasm in both wild-type and *talpid*^{3} cells. These results reinforce the conclusion that the talpid^3 protein is required for efficient processing of functional GliA and GliR but suggest that it is not required for nuclear translocation of these proteins.

Rescue of talpid^3 *neural tube by KIAA0586*

To confirm that KIAA0586 is the *talpid*^{3} gene, we carried out complementation tests. In the first set of experiments, we tested whether KIAA0586 could rescue ectopic induction of dorsoventral markers by Shh in neural tube of stage 17–18 HH *talpid*^{3} embryos. Shh beads were inserted into the neural tube and a pCAGGS-KIAA0586 construct was coelectroporated with a pCAGGS-eGFP control plasmid and dorsoventral patterning examined after 24 h. As noted above, application of a Shh bead to a wild-type neural tube induces ectopic Nkx2.2 (Fig. 7A2, arrows), Islet1 (Fig. 7B2, arrows), shifts strong Pax6 expression dorsally (Fig. 7C2, arrow), induces *Ptc1* throughout the neural tube, surrounding somites, and ectoderm (Fig. 7I) and reduces Pax7 expression ventrally (Fig. 7D2, arrow) while application of Shh to a *talpid*^{3} neural tube has no effect on Nkx2.2, Islet1, Pax6, or Pax7 and only weakly induces *Ptc1* (Supplementary Fig. S6I2,J2, K2,L2,M). When wild-type tissue was electroporated with pCAGGS-KIAA0586 and treated with Shh, a change in gene expression of Nkx2.2, Islet1, Pax6, Pax7, or *Ptc1* was observed on both sides of the neural tube, whether electroporated or not, and therefore attributable only to the effect of the Shh bead (Fig. 7A–D). However,

Downloaded from www.genesdev.org on May 17, 2006

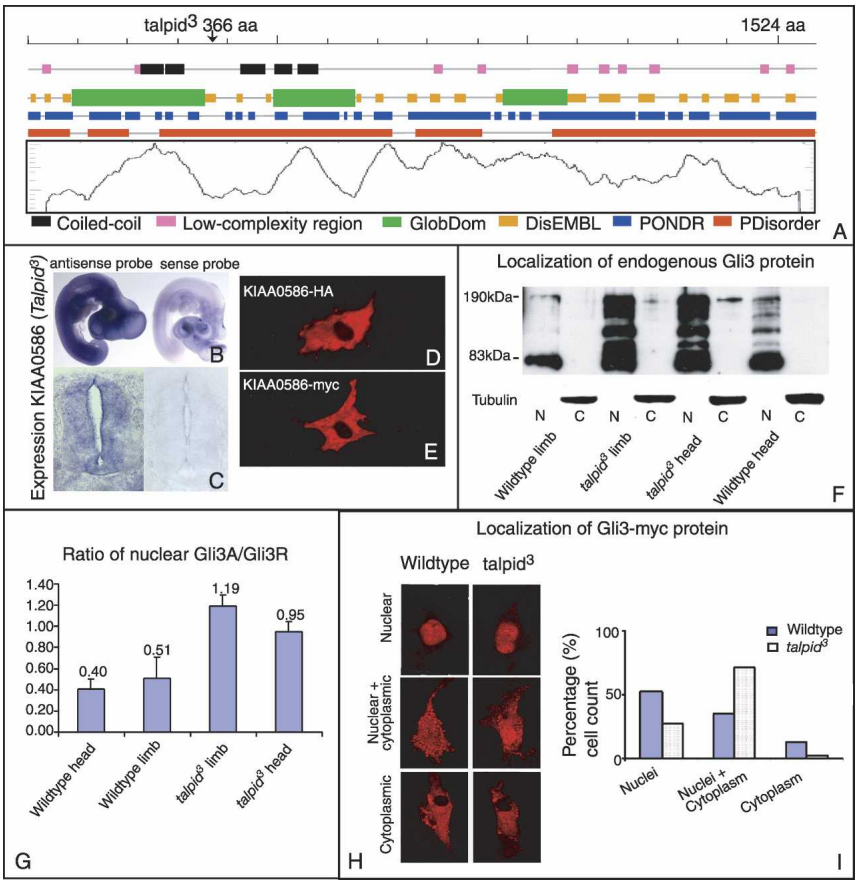

Figure 6. Structure and expression of the talpid^3 protein. (*A*) Wild-type talpid^3/KIAA0586 has 1524 amino acid residues and the *talpid*^{3} gene product is predicted to be only 366 amino acids in length. Predicted regions of low-complexity (pink boxes), coiled-coil domains (black boxes), globular domains (green boxes), and regions of disorder (orange boxes) are shown in the *upper* part of the figure. A similarity plot between vertebrate proteins is shown in the *lower* part of the figure. (*B*) Expression of *KIAA0586* in section of neural tube, stage 20 HH chick embryos, using antisense probe (*left*) and sense probe (*right*) RNA probes. (*C*) Expression of *KIAA0586* in stage 20 HH chicken embryos, using antisense probe (*left*) and sense probe (*right*). (*D*,*E*) Expression in cultured chick mesenchyme cells of pCAGGS-KIAA0586-HA tagged with both HA and Myc. (*D*) Detection of HA. (*E*) Detection of Myc. (*F*) Immunoblot showing localization of Gli3 protein in nuclear (N) and cytoplasmic (C) fractions of cells from wild-type and *talpid*^{3} tissues. (*G*) Histogram comparing the ratios of Gli3A/Gli3R in nuclear extracts made from wild-type and *talpid*^{3} head and limb tissue. (*H*) Expression of myc-Gli3 fusion proteins in *talpid*^{3} and wild-type cells. (*I*) Histograms showing percentage of cells with Gli3 localized in nucleus radius, nucleus and cytoplasm, and cytoplasm only.

when *talpid*^{3} embryos were provided with both Shh and KIAA0586, ectopic expression of Nkx2.2 was induced only on the electroporated side of the neural tube (2/2) (Fig. 7E1–E3, arrows) and in some cells, expression of Pax6 (2/2) (Fig. 7G1,G2, asterisk) and Pax7 was also reduced on the electroporated side (2/2) (Fig. 7H1,H2, asterisk) in a way similar to that seen with Gli3^{HIGH}. Islet1 expression remained unchanged (2/2) (Fig. 7F1,F2). Application of Shh with KIAA0586 also induced high-level *Ptc1* expression in *talpid*^{3} dorsal neural tube on the electroporated side (Fig. 7J; asterisk denotes electroporated side). In preliminary experiments, one *talpid*^{3} embryo had a reduction in Pax7 when electroporated with pCAGGS-KIAA0586 (1/1) (Supplementary Fig. S6H1,H2) but Nkx2.2, Islet1, and Pax6 remained unchanged (Supplementary Fig. S6E–G), and there was no effect on expression of Nkx2.2, Islet1, Pax6, or Pax7 in a wild-type embryo electroporated with pCAGGS-KIAA0586 at stage 17 HH (1/1) (Supplementary Fig. S6A–D).

In a second set of experiments, we tested whether whether KIAA0586 alone could rescue endogenous dorsoventral patterning of the neural tube in very early *talpid*^{3} embryos. In order to carry out these experiments, we had to electroporate batches of embryos from the *talpid*^{3} flock at stages 12–14, well before the mutant phenotype is observable. We electroporated the pCAGGS-KIAA0586 construct, together with pCAGGS-RFP and fixed embryos at stage 20HH in order to examine gene expression. At this stage, we could usually identify mutant embryos by their phenotype, and we confirmed their identity by genotyping. In *talpid*^{3} embryos, we found very striking induction of Islet1 expression (3/3) (Fig. 7K1/2, green cells) coupled with repression of Pax6 (2/2) (Fig. 7L1/2, arrow). We also have preliminary evidence that Pax7 expression was reduced in *talpid*^{3} (1/1) (data not shown). This rescue of endogenous target gene expression provides good evidence that KIAA0568 is the *talpid*^{3} gene and has an essential role in Hh signal transduction.

Discussion

Hh signaling plays crucial roles in development and disease, and therefore it is important to understand the signal transduction pathway that mediates Hh signaling. Here we identify a novel component of the signaling pathway in vertebrates and provide evidence that it is necessary for the function of both Gli repressor and Gli activator forms. By a positional cloning strategy, exploiting the recently assembled chick genome, we provide evidence that *KIAA0586* is the gene responsible for the *talpid*^{3} phenotype. Analysis of KIAA0586 indicates that it contains coiled-coil domains and extensive regions of intrinsic protein disorder (Fig. 6A), characteristic of proteins that play a role in cell signaling and gene regulation

Downloaded from www.genesdev.org on May 17, 2006

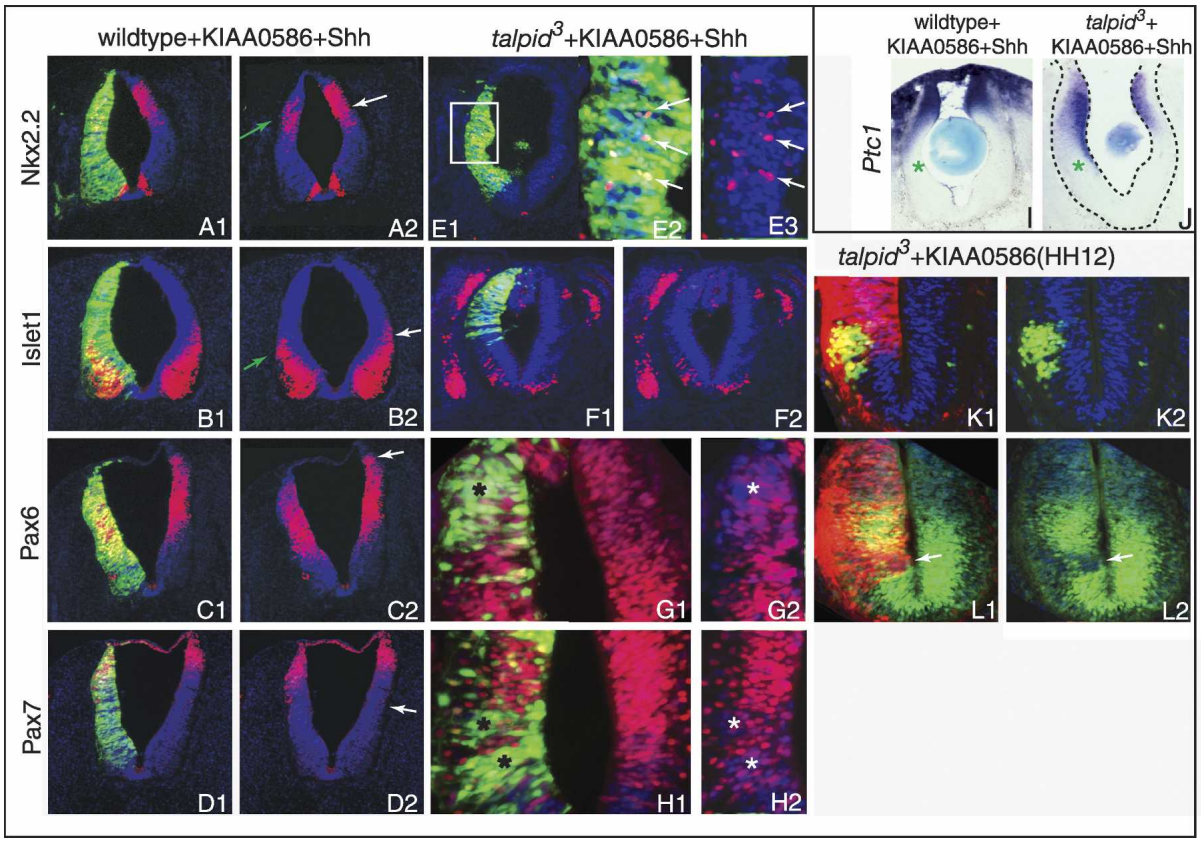

Figure 7. Stage 20 HH wild-type and *talpid*^{3} embryos electroporated with pCAGGS-KIAA0586. In *A–H* green indicates expression of GFP in transfected cells; red indicates protein expression detected by immunohistochemistry. In *K* and *L*, red indicates expression of RFP in transfected cells and green indicates protein expression detected by immunohistochemistry. *K1* and *L1* are overlays of GFP/RFP and immunostaining; *K2* and *L2* are immunostaining alone. (*A–D*) Wild-type neural tube electroporated with pCAGGS-KIAA0586 and treated with Shh. (*A1*,*A2*) Induction of Nkx2.2 in both electroporated and nonelectroporated cells (white arrow, nonelectroporated side; green arrow, electroporated side). (*B1*,*B2*) Expansion of Islet1 in both electroporated and nonelectroporated cells (white arrow, nonelectroporated side; green arrow, electroporated side). (*C1*,*C2*) Pax6 expression dorsalized (arrow) but unaffected by electroporation. (*D1*,*D2*) Pax7 expression dorsalized (arrow) but unaffected by electroporation. (*E–H*) *talpid*^{3} neural tube electroporated with pCAGGS + KIAA0586 and treated with Shh. (*E1–E3*) Nkx2.2 induced only in electroporated cells (arrows). (*F1*,*F2*) Islet1 expression unchanged in both electroporated and nonelectroporated cells. (*G1*,*G2*) Pax6 down-regulated in electroporated cells (asterisk). (*H1*,*H2*) Pax7 down-regulated in electroporated cells (asterisk). (*I*) *Ptc1* induced in somites, ectoderm, and neural tube of wild-type embryos treated with Shh protein independent of pCAGGS-KIAA0586 electroporation (asterisk shows electroporated side). (*J*) *Ptc1* expressed at high levels in *talpid*^{3} cells, both treated with Shh protein and electroporated with pCAGGS-KIAA0586, no expression in surrounding tissue (asterisk electroporated side). *K* and *L* show the results of electroporating *talpid*^{3} embryos at younger stages (HH12–14). (*K1*,*K2*) Islet1 is induced in electroporated cells (yellow/green cells). (*L1*,*L2*) Pax6 expression is lost in electroporated cells (arrow).

(Iakoucheva et al. 2002). Moreover, a frameshift mutation in *KIAA0586* is present in *talpid*^{3} mutants, and the expression of a wild-type *KIAA0586* cDNA in the neural tube of *talpid*^{3} embryos rescued the Shh responsiveness of neural cells and endogenous dorsoventral patterning. We therefore propose that KIAA00586 be renamed Talpid3.

Our analysis of Hh target gene expression in limb, face, neural tube, and somite of *talpid*^{3} embryos, together with our findings that expression of target genes is ligand independent—insensitive to either presence or absence of Shh—and can be rescued by expressing activated Gli are consistent with the idea that both GliA and GliR functions are compromised in *talpid*^{3}. Thus the Talpid3 gene product plays an essential role in both GliA and GliR function in the Hh pathway. The paradoxical *talpid*^{3} phenotype, an apparent mixture of gain and loss of Hh function, is explained by the fact that GliR plays a predominant role in limb and somite, whereas GliA function is more important in face and neural tube patterning.

Our data show that Gli3 processing is impaired in *talpid*^{3} mutant cells, leading to the presence of both full-length Gli3A and Gli3R. Levels of Gli3A, in particular, are markedly increased. Although changes in processing are likely to be the main cause, changes in protein longevity and transcriptional levels could also contribute. The net result is that the ratio of Gli3A/Gli3R is much greater in *talpid*^{3} mutant cells. Abnormal processing is found not only in cells from the limb but also in cells

Downloaded from www.genesdev.org on May 17, 2006

from the trunk, which includes neural tube and somite. We have also shown that, as predicted by its structure, Talpid3 protein is localized in the cytoplasm. Thus, our results are consistent with Talpid3 interacting with other members of the Hh signaling complex to regulate processing of Gli proteins in the cytoplasm. Given the high levels of full-length Gli3, it is not clear why GliA function, in addition to GliR function, is compromised in *talpid*^{3}. This is even more puzzling since we have also shown that the absence of Talpid3 protein does not prevent the ability of Gli3 proteins including Gli3 activator to enter the nucleus. The most likely possibility is that the pathway is very sensitive to the precise levels of full-length and short forms of Gli proteins such that, in the *talpid*^{3} mutant, the levels of GliA and GliR counterbalance their effects, resulting in neither activation nor repression. Alternatively, the Gli3 proteins produced in the absence of Talpid3 may be unable to regulate transcription due to, as yet, unknown post-translational modifications.

Recently two other genes involved in Hh signaling, Dzip1 (Sekimizu et al. 2004; Wolff et al. 2004) (chicken ortholog *ENSGALG00000016895*) and MTSS1 (Callahan et al. 2004) (also called MIM/BEG4, chicken ortholog *ENSGALG00000016333*), have been described. Dzip1 was identified as the Zebrafish mutant gene in the *iguana* mutant, which shows many similarities to the *talpid*^{3} mutant, including reduction of expression of Shh-dependent genes in neural tube coupled with a gain of Hh signaling in the somite. Furthermore, as in *talpid*^{3}, *iguana* cannot be rescued through manipulation of Shh ligand, leading to the suggestion that either both GliA and GliR functions are reduced (Sekimizu et al. 2004), similar to our proposal for *talpid*^{3}, or that GliR fails because of constitutive low-level Gli1 activation (Wolff et al. 2004). There is evidence that Dzip1 can shuttle between cytoplasm and nucleus, and it has been suggested that Dzip1 may affect nuclear import of Hh pathway proteins. This contrasts with Talpid3, which appears to be confined to the cytoplasm and is not required for nuclear import of Gli3. Interestingly, constitutive activation of Shh signaling has been suggested to occur in the *talpid*^{2} chicken mutant (Chuang and McMahon 1999), in which high levels of Gli3A are also found (Wang et al. 2000). *Talpid*^{2}, like *talpid*^{3}, is polydactylous, and the many digits are unpatterned, but, unlike *talpid*^{3}, there is high-level *Ptc* expression throughout the limb (Carrucio et al. 1999), suggesting that Gli activator is functional in this mutant. Thus similarities in phenotype could arise by quite different mechanisms.

A number of intraflagellar transport proteins have been shown to play an essential role in vertebrate Hh signal transduction (Huangfu et al. 2003) in mouse, and a recent report suggests a functional link between Hh signaling and cilia at the level of the transmembrane protein smoothened which is required for GliA function (Corbit et al. 2005). Analysis of hypomorphic mouse mutants of two intraflagellar transport proteins reveals striking parallels between these mutants and *talpid*^{3} (Liu et al. 2005). Not only are the alterations in gene expression patterns in limb and neural tube similar to those seen in *talpid*^{3} and insensitive to Hh ligand, but also high levels of full-length Gli3 were detected in mutant cells, giving rise to a marked increase in the Gli3A/Gli3R ratio. Like Talpid3, intraflagellar transport proteins appear to be required for both GliA and GliR functions. It will be important to determine why mutations in intraflagellar transport proteins compromise GliR function in addition to GliA function and to explore the relationship between Talpid3 and cilia. Talpid3 joins a growing list of proteins, including these intraflagellar transport proteins, that regulate Hh transduction specifically in vertebrates (Chuang and McMahon 1999; Eggenschwiler et al. 2001) and is the first component in this pathway to be discovered in chickens.

Materials and methods

Embryo manipulations

Eggs were incubated for 2.5 d at 38°C, then windowed to assess development and classified as either mutant or wild type and reincubated until the desired stage. All limb manipulations were carried out on the right wing, leaving the left wing as a control.

Cyclopamine treatment: One-hundred microliters of 5 mM cyclopamine in 95% EtOH diluted with 200 µL DMEM was sonicated for 10 min; for the control solution, 100 µL of 95% EtOH was diluted in 200 µL DMEM. Solutions were injected with a fine glass micropipette into the amniotic sac over the right wing of stage 20 HH embryos; eggs were reincubated for 24 h.

Removal of Shh-expressing cells: At stage 16 HH, tissue was removed from flank, immediately lateral to somites, from axial level somites 22 and 18/17 using a sharpened tungsten needle; eggs were then reincubated for 18 h.

RCAS virus production, microinjection, and somite grafts

RCAS virus production and microinjection were done as per Morgan and Fekete (1996). In ovo surgical experiments were performed as per Schmidt et al. (2000), and eggs were reincubated for 40 h.

Tissue graft implants—neural tube

QT-6 Shh expressing cells were grown until confluent. Cell sheets were scraped from the dish surface. A small piece of sheet was folded and tucked into a slit made in the neural tube at the level of the hind limbs using a tungsten needle; eggs were reincubated for 24 h.

Bead implants—neural tube

CM Affi-Gel Blue Beads (Bio-Rad) soaked in Shh protein as per Drossopoulou et al. (2000) were picked up on the point of a tungsten needle and placed into the neural tube via a dorsal slit.

Electroporation

DNA was prepared using a Qiagen Endotoxin-Free Maxiprep Kit, resuspended in endotoxin-free water, and diluted with 0.25% Fast Green. Plasmid pCAGGS-Gli3A^{HIGH} was used at a

Downloaded from www.genesdev.org on May 17, 2006

concentration of 7 µg/µL, pCAGGS-GFP at 7.5 µg/µL, pCAGGS-RFP at 0.1 µg/µL, and pCAGGS-KIAA0586 at 1 µg/µL. DNA was injected into the neural tube and embryos were immediately electroporated at 30 V for 5 × 50 msec with 5 × 50–100-msec intervals or at 20 V for 5 × 15 msec (stages 12–14). Embryos were reincubated for 20–48 h. Successful electroporation was assessed by expression of GFP, eGFP, or RFP using a Leica Fluorescence Dissection Microscope. The GFP section of neural tube was then dissected out in cold PBS (pH 7.4) and fixed for sectioning for immunohistochemistry or whole-mount in situ hybridization.

Whole-mount RNA in situ hybridization

For details, see the Supplemental Material.

Whole-mount immunohistochemistry

For details, see the Supplemental Material.

Section immunohistochemistry

For details, see the Supplemental Material.

Western blotting

For determining levels of Shh protein, stage 20 HH embryo limb buds were dissected into three equal parts along the anterior–posterior axis in cold PBS, lysed in RIPA buffer/1:25 Proteases Inhibitor (Roche), samples ran on 12% SDS-PAGE, and protein detected with Shh antibody. Lysates were spun at 13,000 rpm for 5 min at room temperature, supernatant was removed and methanol precipitated and then dried using the Eppendorf Concentrator. The pellet was resuspended in 30 µL of Sample Buffer 1/10 β-mercaptoethanol and then denatured. Gels were subsequently wet or dry blotted in 1× Tris-Glycine/20%Methanol buffer for 1–2 h at 172 mA onto nitro-cellulose, which was blocked in 5% Marvel/PBS 1:1000 Tween-20; incubated with 1:2 antibody and Marvel/PBT overnight at 4°C; washed 3 h in PBT; incubated in anti-mouse HRP-conjugated (Sigma) in Marvel/PBT 4 h; and washed 1 h in PBT, then 30 min in PBS. Detection was with Supersignal West Pico Chemiluminescent Substrate (Pierce) for 5 min and was detected with X-ray film exposed overnight.

Levels of full-length and short forms of Gli3 protein were determined in protein extracts from limb buds and trunks dissected from stage HH24 embryos. Some limb buds were dissected into three equal parts as above. All tissues were then lysed in buffer containing 1% NP-40, 150 mM NaCl, and 20 nM Tris (pH 7.4) in the presence of Complete protease inhibitor cocktail (Roche). Protein concentrations were measured using Bradford (Pierce), and equal amounts of protein were separated by SDS-PAGE using 4%–12% precast gels from Invitrogen. Immunoblot was performed using a polyclonal antibody against Gli3 (Santa Cruz Biotechnology, Inc).

Nuclear and cytosol fractionation

Limbs and heads from stage 24HH embryos were dissected out in cold PBS and cut into small pieces with scissors. Homogenization of tissue was carried out by a pestle on ice. Extraction of nuclear and cytoplasmic fractions was performed using a Compartmental Protein extraction Kit (Chemicon) as per the manufacturer's instruction. Protein concentration was determined by the Bradford method. Nuclear and cytoplasmic fractions were stored at –80°C for Western blot analysis.

Cell cultures and immunohistochemistry

DFI chicken cells were grown in DMEM + 10% fetal calf serum; constructs containing either KIAA0586-myc or KIAA0586-HA were introduced using FuGene (Roche).

Primary cell culture and immunofluorescence staining

Individual chick limbs from HH20–24 embryos were dissected in sterile cold PBS and incubated with 1× Trypsin and EDTA for <5 min at 37°C. A 20-µL cell suspension was plated onto cover glasses coated by fibronectin. The cover glasses were set in a Petri dish and incubated at 37°C for an hour followed by flooding cells with 1:1, DMEM-HAMS F12/10% FCS, 1% PSF, 1% L-glutamine. The next day, cells were transfected with myc-hGli3 or KIAA0586-myc or KIAA0586-HA using FuGene 6 (Roche).

After 24 h transfection, cells were washed in PBS, fixed in ice-cold methanol for 10 min, then blocked in 10% normal serum in PBS for 30 min. Cells were incubated in monoclonal anti-c-myc (1:1000, Sigma) 1 h at room temperature, washed 3 × 5 min in 0.2% Tween-20 in PBS, and incubated in anti-mouse IgG conjugated with Alexa Fluor 610 (1:1000, Molecular Probes) for 1 h at room temperature. After washes (3 × 5 min in 0.2% Tween-20 in PBS), cells were mounted in VectaShield Hard*set mount medium with DAPI (Vector Laboratories, H-1500). Fluorescence was observed using a fluorescence microscope or a Leica SP2 confocal microscope.

Animals and genetic linkage analysis

Talpid^3 carriers were maintained by outcrossing with ISA Brown chickens. Line 6, an inbred White Leghorn line, was kindly provided by the Institute of Animal Health (Compton). A male carrier (*TA3/N*) was crossed to eight Line 6 females (*N/N*) and offspring of this backcross were test-crossed with known carriers. A carrier was confirmed if two or more *talpid*^{3} embryos were found from a test cross. At least 20 wild-type embryos were collected before any noncarriers were confirmed. Four DNA pools were created from backcross offspring: Carrier male (n = 13), carrier female (n = 32), noncarrier male (n = 7), and noncarrier female (n = 16) were genotyped using 129 autosomal genetic markers, covering 70% of the genome. Markers *ADL0298* and *ADL0166* on chromosome 5 showed a significant difference ($p < 0.00001$) between carrier and noncarrier pools. Further markers near these loci were used to genotype 110 individuals and refine the location of the *TA3* locus. Two-point and multipoint linkage analysis was performed using CRIMAP (Green et al. 1990). From this analysis, 30 recombinant offspring were identified near *TA3* between markers *ADL0166* and *ADL0298* and typed using markers developed from EST and genomic sequences. Using known chicken genes and reference to the Ensembl (http://www.ensembl.org) and University of California at Santa Cruz (http://www.genome.ucsc.edu) genome browsers, we identified the orthologous region on human chromosome 14. Using human gene sequences and Blast we searched databases (http://www.ncbi.org) for homologous chicken EST and genomic sequences. We developed PCR-based markers from these showing size and SSCP or SNP variation. These markers were used to isolate and order individual BAC clones (Burt et al. 2003) to create a detailed physical map. BAC-end and full-length cDNA sequences were also used to create more genetic markers. Using such a high density of markers we were able to identify specific haplotypes from recombinants in this region and map the *TA3* locus to *KCNK16-DACT1-KIAA0586-TIMM9-ARID4A*. Genotyping was performed as described by Burt et al. (2003) and primers used for genotyping are listed in Supplementary Table S2.

Downloaded from www.genesdev.org on May 17, 2006

Sequence analysis and characterization of talpid^3 *mutation*

For details, see the Supplemental Material.

Genotyping

Genomic DNA was prepared from extra-embryonic membranes using Quigen DNAeasy Kit. A 957-base-pair (bp) region of the *talpid*^{3} gene was then amplified via PCR (forward: CTTCTCT TGCCCTGCCTTAC; reverse: TTGAAGCTGCATTTCCA CAG), annealed at 60°C (Thermo electron) using Fast Start Taq Polymerase and GC-rich solution (Roche). The PCR product was then digested using Pst1 (Roche). A single 957-bp band indicates a wild-type embryo, two bands (721 bp and 236 bp) indicate a *talpid*^{3} mutant, and three bands indicate a heterozygous embryo.

Cloning of chicken cDNA clones and gene constructs

RNA was extracted using TRIzol reagent (Invitrogen), and a DACT1 cDNA was cloned via RT–PCR (P1: GGGATGCTG GCCTATTAAATC in exon 2; P2: GCTTCCCAAAG CAGAAACAG, in 3′ UTR) from embryo-derived mRNA (HH stage 21) using the TOPO TA cloning kit (Invitrogen), then subcloned into pGEM (Invitrogen) for preparation of antisense RNA probes. Rapid amplification of 5′ cDNA ends of *KIAA0586* and *DAAM1* was carried out using the First Choice RLM-RACE Kit (Ambion) and cloned using the TOPO TA cloning kit. Gene-specific primers are listed in Supplementary Table S2.

Bioinformatics analyses

For details, see the Supplemental Material.

Accession numbers

All sequences have been deposited in GenBank under accession numbers DQ066927–DQ066935 and CZ550237–CZ550250.

Acknowledgments

We are grateful to Dr. Jun-ichi Miyazaki and Dr. Toshihiko Agura for providing pCAGGS-eGFP, Dr. Ruiz i Altaba for plasmid myc-hGli-3, Dr. R. Johnson and Dr. C. Tabin for pRCAS-Shh, Professor Groenen for chicken BAC clones, and Dr. Placzek for Shh antibody. EST clones from UK Chick EST Project were provided by ARK-Genomics (http://www.ark-genomics.org). This research was supported by the BBSRC (to M.D., I.R.P., Y.Y., D.R.M., F.K.B., D.R.M., D.B., and C.T.), British Heart Foundation (to M.D. and C.T.), MRC (UK; to T.G.S., M.T. and C.T.), and The Royal Society (to T.G.S. and C.T.). D.S. and J.B. were supported by the MRC (UK) and an EC network grant Stembridge (QLG3-CT-2002-011441); A.E.M. and M.S. were supported by The Wellcome Trust and MYORES (EU FP6 NoE).

References

Bai, C.B., Auerbach, W., Lee, J.S., Stephen, D., and Joyner, A.L. 2002. Gli2, but not Gli1, is required for initial Shh signaling and ectopic activation of the Shh pathway. *Development* **129:** 4753–4761.

Borycki, A.G., Brunk, B., Tajbakhsh, S., Buckingham, M., Chiang, C., and Emerson, C.P.J. 1999. Sonic hedgehog controls epaxial muscle determination through Myf5 activation. *Development* **126:** 4053–4063.

Burt, D.W., Morrice, D.R., Lester, D.H., Robertson, G.W., Mohammed, M.D., Simmons, J., Downey, L.M., Thuang, C., Bridges, L.R., Paton, I.R., et al. 2003. Analysis of rdd locus in chicken: A model for human retinitis pigmentosa. *Mol. Vis.* **9:** 164–170.

Buxton, P., Davey, M.G., Paton, I.R., Morrice, D.R., Francis-West, P.H., Burt, D.W., and Tickle, C. 2004. Craniofacial development in the *talpid3* chicken mutant. *Differentiation* **72:** 348–362.

Callahan, C.A., Ofstad, T., Horng, L., Wang, J.K., Zhen, H.H., Coulombe, P.A., and Oro, A.E. 2004. MIM/BEG4, a Sonic hedgehog-responsive gene that potentiates Gli-dependent transcription. *Genes & Dev.* **18:** 2724–2729.

Carrucio, N.C., Martinez-Lopez, A., Harris, M., Dvorak, L., Bitgood, J., Simandl, B.K., and Fallon, J.F. 1999. Constitutive activation of sonic hedgehog signaling in the chicken mutant talpid2, Shh independent outgrowth and polarizing activity. *Dev. Biol.* **212:** 137–149.

Chuang, P.T. and McMahon, A.P. 1999. Vertebrate Hedgehog signaling modulated by induction of a Hedgehog-binding protein. *Nature* **397:** 617–621.

Corbit, K.C., Aanstad, P., Singla, V., Norman, A.R., Stainier, D.Y., and Reiter, J.F. 2005. Vertebrate Smoothened functions at the primary cilium. *Nature* **437:** 1018–1021.

Drossopoulou, G., Lewis, K.E., Sanz-Ezquerro, J.J., Nikbakht, N., McMahon, A.P., Hofmann, C., and Tickle, C. 2000. A model for anteroposterior patterning of the vertebrate limb based on sequential long- and short-range Shh signaling and Bmp signaling. *Development* **127:** 1337–1348.

Ede, D.A. and Kelly, W.A. 1964a. Developmental abnormalities in the head region of the talpid mutant of the fowl. *J. Embryol. Exp. Morphol.* **12:** 161–182.

———. 1964b. Developmental abnormalities in the trunk and limbs of the fowl. *J. Embryol. Exp. Morphol.* **12:** 339–356.

Eggenschwiler, J.T., Espinoza, E., and Anderson, K.V. 2001. Rab23 is an essential negative regulator of the mouse Sonic hedgehog pathway. *Nature* **412:** 194–198.

Francis-West, P.H., Robertson, K.E., Ede, D.A., Rodriguez, C., Izpisua-Belmonte, J.C., Houston, B., Burt, D.W., Gribbin, C., Brickell, P.M., and Tickle, C. 1995. Expression of genes encoding bone morphogenetic proteins and sonic hedgehog in talpid (ta3) limb buds: Their relationships in the signaling cascade involved in limb patterning. Dev. Dyn. **203:** 187–197.

Frank-Kamenetsky, M., Zhang, X.M., Bottega, S., Guicherit, O., Wichterle, H., Dudek, H., Bumcrot, D., Wang, F.Y., Jones, S., Shulok, J., et al. 2002. Small-molecular modulators of Hedgehog signaling: Identification and characterization of Smoothened agonists and antagonists. *J. Biol.* **1:** 10.

Green, P., Falls, K., and Crooks, S. 1990. *Documentation for CRIMAP, version 2.4*. Washington School of Medicine, St. Louis, MO.

Hamburger, V. and Hamilton, H.L. 1951. A series of normal stages in the development of the chick embryo. *J. Morphol.* **88:** 49–92.

Hinchliffe, J.R. and Ede, D.A. 1968. Abnormalities in bone and cartilage development in the talpid mutant of the fowl. *J. Embryol. Exp. Morphol.* **19:** 327–339.

Huangfu, D., Liu, A., Rakeman, A.S., Murcia, N.S., Niswander, L., and Anderson, K.V. 2003. Hedgehog signaling in the mouse requires intraflagellar-transport proteins. *Nature* **426:** 83–87.

Hui, C.C. and Joyner, A.L. 1993. A mouse model of greig cephalopolysyndactyly syndrome: The extra-toesJ mutation contains an intragenic deletion of the Gli3 gene. *Nat. Genet.* **3:** 241–246.

Downloaded from www.genesdev.org on May 17, 2006

Hunton, P. 1960. "A study of some factors affecting the hatchibility of chicken eggs, with special reference to genetic control." MSc. thesis, Wye College, University of London, UK.

Iakoucheva, L.M., Brown, C.J., Lawson, J.D., Obradovic, Z., and Dunker, A.K. 2002. Intrinsic disorder in cell-signaling and cancer-assoicated proteins. *J. Mol. Biol.* **323:** 573–584.

Ingham, P.W. and McMahon, A.P. 2001. Hedgehog signaling in animal development, paradigms and principles. *Genes & Dev.* **15:** 3059–3087.

International Chicken Genome Sequencing Consortium 2004. Sequence and comparative analysis of the chicken genome provide unique perspectives on vertebrate evolution. *Nature* **432:** 695–716.

Izpisua-Belmonte, J.C., Ede, D.A., Tickle, C., and Duboule, D. 1992. The mis-expression of posterior Hox-4 genes in talpid (ta3) mutant wings correlates with the absence of anteroposterior polarity. *Development* **114:** 959–963.

Lewis, K.E., Drossopoulou, G., Paton, I.R., Morrice, D.R., Robertson, K.E., Burt, D.W., Ingham, P.W., and Tickle, C. 1999a. Expression of ptc and gli genes in talpid3 suggests bifurcation in Shh pathway. Development **126:** 2397–2407.

Lewis, K.E., Currie, P.D., Roy, S., Schauerte, H., Haffter, P., and Ingham, P.W. 1999b. Control of muscle cell-type specification in the zebrafish embryo by Hedgehog signaling. *Dev. Biol.* **216:** 469–480.

Litingtung, Y., Dahn, R.D., Li, Y., Fallon, J.F., and Chiang, C. 2002. Shh and Gli3 are dispensable for limb skeleton formation but regulate digit number and identity. *Nature* **418:** 979–983.

Liu, A., Wang, B., and Niswander, L.A. 2005. Mouse intraflagellar transport proteins regulate both the activator and repressor functions of Gli transcription factors. *Development* **132:** 3103–3111.

Morgan, B.A. and Fekete, D.M. 1996. Manipulating gene expression with replication-competent retroviruses. *Methods Cell Biol.* **51:** 185–218.

Munsterberg, A.E., Kitajewski, J., Bumncrot, D.A., McMahon, A.P., and Lassar, A.B. 1995. Combinatorial signaling by Sonic hedgehog and Wnt family members induces myogenic bHLH gene expression in the somite. *Genes & Dev.* **9:** 2911–2922.

Pearse, R.V., Vogan, K.J., and Tabin, C.J. 2001. Ptc1 and Ptc2 transcripts provide distinct readouts of Hedgehog signaling activity during chick embryogenesis. *Dev. Biol.* **239:** 15–29.

Persson, M., Stamataki, D., te Welscher, P., Andersson, E., Bose, J., Ruther, U., Ericson, J., and Briscoe, J. 2002. Dorso-ventral patterning of the spinal cord requires Gli3 transcriptional repressor activity. *Genes & Dev.* **16:** 2865–2878.

Rat Genome Sequencing Project Consortium 2004. Genome sequence of the Brown Norway rat yields insights into mammalian evolution. *Nature* **428:** 493–521.

Ruiz i Altaba, A., Nguyen, V., and Palma, V. 2003. The emergent design of the neural tube, pre-pattern, SHH morphogen and GLI code. *Curr. Opin. Genet. Dev.* **13:** 513–521.

Schmidt, M., Tanaka, M., and Munsterberg, A. 2000. Expression of β-catenin in the developing chick myotome is regulated by myogenic signals. *Development* **127:** 4105–4113.

Sekimizu, K., Nishioka, N., Sasaki, H., Takeda, H., Karlstrom, R.O., and Kawakami, A. 2004. The Zebrafish iguana locus encodes Dzip1, a novel zinc-finger protein required for proper regulation of Hedgehog Signaling. *Development* **131:** 2521–2532.

Stamataki, D., Ulloa, F., Tsoni, S.V., Mynett, A., and Briscoe, J. 2005. A gradient of gli activity mediates graded Sonic Hedgehog signaling in the neural tube. *Genes & Dev.* **19:** 626–641.

te Welscher, P.T., Zuniga, A., Kuijper, S., Drenth, T., Goedemans, H.J., Meijlink, F., and Zeller, R. 2002. Progression of vertebrate limb development through SHH-mediated counteraction of GLI3. *Science* **298:** 827–830.

Wang, B., Fallon, J.F., and Beachy, P.A. 2000. Hedgehog-regulated processing of Gli3 produces an anterior/posterior repressor gradient in the developing vertebrate limb. *Cell* **100:** 423–434.

Wolff, C., Roy, S., Lewis, K.E., Schauerte, H., Joerg-Rauch, G., Kim, A., Weiler, C., Geisler, R., Haffter, P., and Ingham, P. 2004. Iguana encodes a novel zinc-finger protein required for proper regulation of Hedgehog Signaling. *Development* **131:** 2521–2532.

Yang, Z. and Nielsen, R. 2000. Estimating synonymous and nonsynonymous substitution rates under realistic evolutionary models. *Mol. Biol. Evol.* **17:** 32–43.